JACS
JOURNAL OF THE AMERICAN CHEMICAL SOCIETY
Communication
pubs.acs.org/JACS

# Direct Evidence for Single-Crystal to Single-Crystal Switching of Degree of Interpenetration in a Metal–Organic Framework

Himanshu Aggarwal, Prashant M. Bhatt, Charl X. Bezuidenhout, and Leonard J. Barbour*

Department of Chemistry and Polymer Science, University of Stellenbosch, Matieland 7602, Stellenbosch, South Africa

Supporting Information

**ABSTRACT:** A known doubly interpenetrated metal–organic framework with the formula $[Zn_2(ndc)_2(bpy)]$ possesses minimal porosity when activated. We show not only that the material converts to its triply interpenetrated analogue upon desolvation, but also that the transformation occurs in a single-crystal to single-crystal manner under ambient conditions. The mechanism proposed for the conversion is supported by computational methods and by analogy with the solid-state behavior of an analogous system.

One of the primary goals of crystal engineering is to understand structure–function relationships at the molecular level,[1] with a view to establishing protocols for the development of designer materials. Some of these materials might be exploited as single-crystal devices, in which case it would generally be desirable for a crystal to undergo nondestructive internal changes in order to perform a specific function.[2,3] For example, a single crystal of a porous framework has recently been used for structural characterization of nanogram quantities of scarce natural products, thereby establishing a new approach to the characterization of very small quantities of compound that cannot be characterized by means of conventional analytical techniques.[4] Owing to the requirement for three-dimensional packing periodicity of their components, crystals usually crack or crumble as a result of the long-range strain introduced when the internal periodicity is disrupted. Therefore, we refer to crystals as being brittle unless the internal changes can be effected in a concerted fashion that preserves molecular-level continuity throughout the single-crystal phase transformation (SCPT). Discrete crystals have been shown to tolerate considerable dynamic behavior at the molecular level while maintaining their single-crystal character. Examples that are common in the literature include bond formation/cleavage,[5] guest uptake,[6,7] release,[6] or exchange[8] as well as polymorphic phase transformations.[9] Although occurrences of SCPTs are usually anecdotal, it has become interesting to probe the extent to which structural changes might occur within crystals without destroying their macroscopic integrity.

Because of their numerous potential applications, metal–organic frameworks (MOFs) and related materials are of considerable interest in chemistry and materials science.[10−12] Accordingly, much effort has been devoted to structural aspects of MOFs with a view to gaining better understanding and control of their properties. In particular, the use of structurally robust secondary building units (SBUs) that are based on metal clusters is a common approach toward the reticular synthesis of MOF materials that maintain their framework connectivity after solvent removal, often even surviving as single crystals.[13] Indeed, this strategy has become routine for the preparation of numerous porous materials. Framework interpenetration is a well-known structural feature in MOFs and related structures;[11,14−16] when the open spaces of a network are large enough, one or more additional (usually identical) networks can be accommodated within these spaces such that there are no formal bonds between the different networks. This means that the networks cannot be separated without breaking numerous chemical bonds,[15] and the degree of interpenetration may be 2-fold or greater, subject to the grid dimensions. Whether interpenetration is welcomed or unwanted depends upon the desired properties of the material. For example, interpenetration can promote flexibility in MOFs, resulting in dynamic phenomena that can be exploited for selective guest capture and separation.[14,16] On the other hand, interpenetration reduces the guest-accessible volume, and it is one of the major obstacles to preparing MOFs with large surface areas.[15,17,18] Either way, interpenetration cannot be ignored, and a better understanding of this important phenomenon would be helpful in designing dynamic materials with tailor-made properties.

As part of our exploration of pillared-layer structures, we have reinvestigated a system composed of naphthalene dicarboxylic acid (ndc), 4,4′-bipyridine (bpy), and the zinc paddlewheel SBU. There have been two independent reports of this system based on single-crystal diffraction (SCD) analysis—one describing a 2-fold (**2f**)[19] and the other a 3-fold (**3f′**)[20] interpenetrated structure, both with the network formula $[Zn_2(ndc)_2(bpy)]$. The crystal structure of **2f** (Figure 1a,b) possesses 44% guest-accessible volume and contains dimethylformamide (DMF) and water molecules in channels, although the guest solvent could not be modeled. In contrast, the structure of **3f′** possesses much less guest-accessible space (18%) and thus fewer solvent molecules (also not modeled).[20] We prepared crystals of **2f**, and thermogravimetric analysis (TGA) shows a 25% weight loss in the temperature range 40–140 °C, which corresponds to three DMF molecules and one $H_2O$ molecule per formula unit (see Supporting Information (SI), Figure S10a). In order to remove the solvent from **2f** for subsequent porosity studies, crystals were subjected to dynamic vacuum at 120 °C for 24 h. Although many of the crystals

**Received:** January 17, 2014
**Published:** February 20, 2014

   dx.doi.org/10.1021/ja500530y | J. Am. Chem. Soc. 2014, 136, 3776–3779

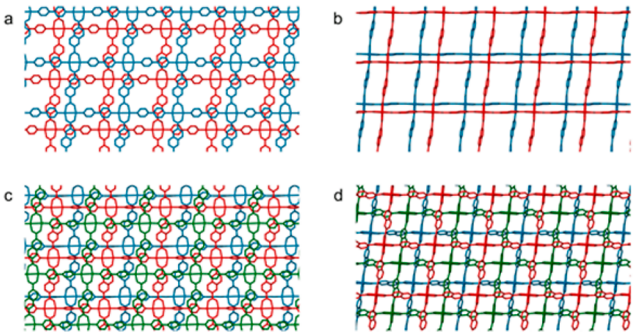


**Figure 1.** Structure of doubly interpenetrated [Zn2(ndc)2(bpy)] (**2f**) viewed perpendicular to the (a) (100) and (b) (001) planes converts in single-crystal to single-crystal fashion to **3f** viewed perpendicular to the (c) (110) and (d) (001) planes. Guest DMF molecules, hydrogen atoms and disordered components have been omitted for clarity. The independent frameworks are colored red and blue for **2f** and red, green, and blue for **3f**. In all cases the ligands propagating the frameworks in the direction of the projection have been omitted.

became opaque upon desolvation, several SCD-quality crystals remained intact.

Remarkably, SCD analysis of these crystals revealed a new 3-fold interpenetrated structure **3f** (Figure 1c,d), which is different from that reported in the literature (i.e., **3f′**).[20] The structure of **3f** is reminiscent of **3f′**, having the same SBU and metal to ligand connectivity, but it possesses 17% guest-accessible volume within which it was still possible to model DMF guest molecules (0.4 molecule of DMF per formula unit). A comparison of the powder X-ray diffraction (PXRD) patterns of the simulated structures of **3f** and **3f′** shows that these two phases are easily distinguishable from each other (Figure S17). There are also small differences in dihedral angles of the ligands and the coordination angles, and the crystallographic symmetry is also different for the two structures. PXRD analysis of the desolvated bulk sample matched the pattern simulated from the SCD structure (see SI) of as-synthesized **3f**. Indeed, the desolvation experiment was repeated several times and under different conditions, and in each case PXRD analysis confirmed full conversion of **2f** to **3f** (see SI). We also observed that **2f** converts to **3f** upon standing under ambient conditions (i.e., in the absence of mother liquor), as verified by unit cell determinations (see SI). This implies that the transformation follows a relatively low energy pathway as compared to a previous report of a change in interpenetration resulting from extreme heating of the material.[21] Moreover, in this particular case the change in interpenetration results from spontaneous loss of DMF guest molecules from the channels which, in turn, leads to spontaneous conversion of the structure from **2f** to **3f**. The previously reported example involved complete removal of the ligand upon heating, leading to a change in the coordination environment around the metal atom, whereas in the present case the coordination environment remains the same even after conversion.

In order to show unequivocally that the conversion occurs as a SCPT, it is highly desirable to carry out complete SCD structural analyses of the same crystal both before and after transformation. A single crystal of **2f** was glued to a glass fiber and inserted into a Lindeman glass capillary with an outer diameter of 0.3 mm and a wall thickness of 10 $\mu$m. The crystal was thermostated at 200 K while X-ray intensity data were collected, yielding the structure of **2f**. The temperature was then increased to 298 K at a rate of 120 K $h^{-1}$ and kept constant while the unit cell was determined repeatedly. After approximately 6 h at 298 K, unit cell determination indicated that the transformation to **3f** had occurred to near completion (i.e., the unit cell could only be indexed as that of **3f**). The temperature was then decreased back to 200 K, and X-ray diffraction data were collected once again, yielding the structure of **3f**. It is noteworthy that the crystal quality did not deteriorate as a result of the SCPT, as verified by visual inspection and measurement of its mosaicity (see SI). Conversion of **2f** to **3f** was also investigated using other techniques. Optical microscopy revealed substantial reduction in the crystal size upon desolvation over time, which is consistent with conversion of **2f** to **3f** (Figure S14). Time-lapse solid-state UV−visible spectroscopy also indicated a gradual change from **2f** to **3f** upon desolvation—a reflectance band around 225 nm started appearing after 2 h and gradually increased in intensity over time. After 24 h the spectrum did not change any further and matched that of **3f** prepared by heating **2f** under vacuum (Figures S12 and S13). In order to investigate the reversibility of the transformation **2f**→**3f**, a transformed crystal of **3f** was immersed in DMF at room temperature for 24 h. Determination of the unit cell parameters did not indicate reversion to **2f**. When the experiment was then repeated at 120 °C, the same result was obtained. Similar experiments were carried out using powdered material (see SI), and it does not appear that the transformation is reversible under the conditions investigated.

The well-studied benzene dicarboxylic acid (bdc) analogue of the $[Zn_2(ndc)_2(bpy)]$ system may offer clues toward suggesting a plausible mechanism for the conversion of the latter from **2f** to **3f**. $[Zn_2(bdc)_2(bpy)]$ is also formed as a DMF solvate ($\mathbf{1}_{DMF}$) under solvothermal conditions. On heating under dynamic vacuum, $\mathbf{1}_{DMF}$ converts to the desolvated nonporous phase (**1**).[22] The most conspicuous difference between $\mathbf{1}_{DMF}$ and **1** involves the coordination geometry of the bpy ligand: the (Zn···Zn)−N bond angle in $\mathbf{1}_{DMF}$ is almost linear (ca. 176°), and in **1** it becomes considerably bent (ca. 153°). It appears that this angular distortion occurs in order to minimize the empty space in the desolvated structure. The structure of **2f** is quite similar to that of $\mathbf{1}_{DMF}$, except that ndc is longer than bdc, and hence the grid spacing and channel sizes are larger in the case of **2f**. Extending the analogy, upon desolvation of **2f**, the corresponding coordination angle of the bpy linker should also distort in order to reduce the amount of empty space. Indeed, it is reasonable to expect even more severe distortion of the (Zn···Zn)−$N_{bpy}$ angle in the case of **2f**→**3f** owing to the greater solvent-accessible volume of **2f** relative to that of **1**. We therefore postulate a transformation mechanism based on the assumption that the ndc carboxylate-linked layers are able to slide laterally while maintaining their connectivity during the conversion, whereas the bpy pillars can undergo Zn−N bond cleavage and re-formation (see video file in SI).

With reference to Figure 2, the two frameworks in the structure of **2f** are offset with respect to each other such that they contain guest-accessible space (1), with the guest molecules playing a structure-supporting role. With respect to the stacking direction (i.e., the vertical direction in Figure 2), pairs of proximate adjacent layers (i.e., bilayers) from the two distinct networks slide laterally and in unison as the guest molecules are driven from the crystals (2). This transverse displacement is facilitated by the ability of the bpy pillars to become distorted until they reach the limit at which the Zn−N


dx.doi.org/10.1021/ja500530y | J. Am. Chem. Soc. 2014, 136, 3776−3779

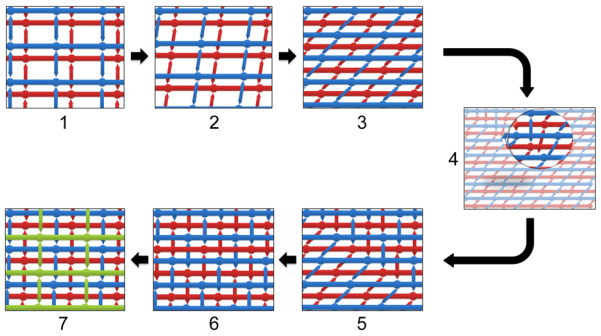


**Figure 2.** Schematic representation of the suggested mechanism governing the conversion from **2f** to **3f**. Independent frameworks are colored red, green, and blue. The $Zn_2$ cluster SBUs are represented by circles, the ndc linkages by solid lines, and the bpy linkages by double-ended arrows. In the projections shown, the ndc-linked layers form horizontal planes that are pillared in the vertical direction by means of bpy ligands.

coordination bonds can still be maintained (3). Since the bilayers are tethered to their neighboring bilayers by means of the bpy pillars, this sliding motion brings the bilayers closer together until all of the ndc-linked planes are approximately evenly spaced. Owing to enforced instability of the distorted Zn−N linkages, the bpy ligands each begin to detach from one of their associated Zn ions and reattached to a more favorably located metal site to once again form an almost linear (Zn···Zn)−bpy−(Zn···Zn) pillared connection (4, inset). Ultimately this mechanism should cascade through the crystal (5) until all of the bpy connections have been reassigned (6). The final result of this process is that the doubly interpenetrated ***...ababab...*** layers of ndc-linked SBUs in **2f** (shown respectively as ***a*** = red and ***b*** = blue in 1−3) become triply interpenetrated ***...abcabc...*** layers (red, blue, and green in 7) as a result of the new interconnections by means of the bpy pillars. We note that a SCPT involving substantial lateral translation (by approximately 6 Å) of layers relative to one another has previously been observed in an organic crystal.[23] The zinc paddlewheel SBU is generally considered to be flexible, but still sufficiently robust not to undergo bond cleavage or rearrangement during crystal desolvation, and a recent report[24] describing the internal rearrangement of a paddlewheel SBU represents by far the most dramatic distortion observed heretofore. However, to date there has been no unequivocal report describing a change in network connectivity involving metal-cluster SBUs as a SCPT. That such a process can occur throughout a single crystal without causing fracturing is surprising since it requires a high degree of internal cooperativity to be maintained throughout the transformation process.

The proposed mechanism is also supported by computational methods; the model used to investigate the relationship between a bpy pillar and a zinc-ndc paddlewheel node is shown in Figure 3a. Using the geometry in **2f** as the starting point, an angular scan was carried out by incrementally tilting the bpy molecule (i.e., by manipulating its angle $\phi$, Figure 3b). The system was allowed to optimize after each step using the positions of each preceding step as a starting point, and plots of the resulting Zn1−N1 coordination bond length, the bpy inclination angles ($\theta$ and $\phi$), and the corresponding energy of the system are shown in Figure 3c,d. The angle $\theta$ decreases with decreasing $\phi$ (Figure 3d), with concomitant lengthening of the Zn−N bond, as evidenced by the increasing relative

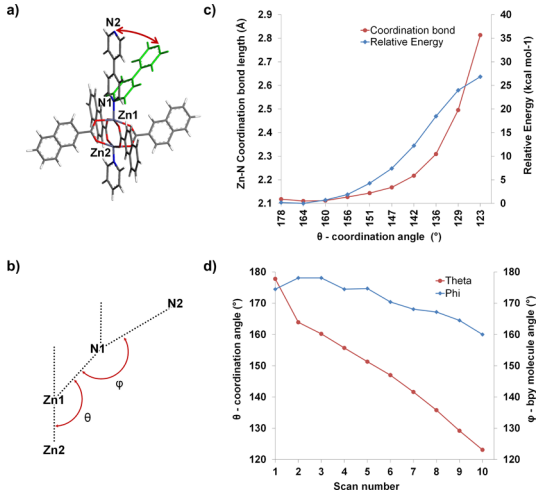


**Figure 3.** Change in the energy of the system with deformation of the $(Zn\cdots Zn)-N_{bpy}$ orientation. (a) The model used for an angular scan of the $(Zn\cdots Zn)-N_{bpy}$ bond angle by rotating the bpy molecule in steps of 2.5° over 20 steps. (b) Diagrammatic representation of the bpy coordination ($\theta$) and ligand orientation ($\varphi$) angles. (c) Plot of the change in the N1−Zn1 coordination bond length and the energy of the system with decreasing $\theta$. (d) Change in the coordination and ligand angles $\theta$ and $\varphi$ with scan step number.

energy of the system (Figure 3c). Moreover, as $\varphi$ deviates further from linearity, the $(N\cdots N)_{bpy}$ axis gradually points away from the metal, thus further destabilizing the coordination bond. Since the relative energy of the system increases approximately exponentially, it seems reasonable to assume that distortion of the (Zn···Zn)−bpy−(Zn···Zn) geometry will ultimately result in bond cleavage, followed by formation of a more favorable connection between the freed extremity of the bpy ligand and a different metal center.

Although a few recent reports have mentioned changes in the degree of interpenetration of MOFs upon desolvation, the transformations have always occurred with concomitant polycrystalline degradation of single crystals.[25,26] However, to our knowledge the present study is the first unequivocal description of a change in the degree of interpenetration occurring as a single-crystal to single-crystal phase transformation, as verified by structural analysis of the same crystal both pre- and post-conversion. The relative ease with which **2f** converts to **3f** suggests that many more such conversions might be possible, but they have most likely not been reported because the crystal structure of the desolvated phase has not yet been determined; i.e., in most of the cases single crystals do not survive substantial rearrangement during such conversions, making structural analysis difficult to accomplish. Researchers in this area often encounter instances in which the surface area of a material is much lower than expected from SCD analysis of the original open framework,[19,27−30] or the material irreversibly converts to an unknown nonporous (or collapsed) phase upon desolvation. A report by Hupp and co-workers on **2f** and its sorption properties stated that "$N_2$ adsorption measurements on framework **3** [evacuated **2f**] yields a lower than anticipated surface area due to possible channel collapse".[19] We have now established that the evacuated "framework **3**" is actually **3f** and that the channels do not merely collapse; instead, complete transformation of the structure takes place from the highly porous doubly interpenetrated **2f** to the considerably less porous triply interpenetrated **3f**, the structure of which was not


dx.doi.org/10.1021/ja500530y | J. Am. Chem. Soc. 2014, 136, 3776−3779

previously known. Another report[31] compared the PXRD patterns of evacuated **2f** with analogous structures that are 3-fold interpenetrated but provided no evidence for the transformation of **2f** to **3f** as a SCPT. The present study not only provides direct evidence for a change in degree of interpenetration but also emphasizes that this phenomenon should also be considered as a very plausible possibility when explaining the loss of porosity in MOFs upon desolvation. Indeed, in this context we examined the previously reported[28] doubly interpenetrated *trans*-1,2-bis(4-pyridyl)ethylene (bpe) analogue of **2f**, since it has been reported that the surface area of $[Zn_2(ndc)_2(bpe)]$ is much lower than expected from the crystal structure of the solvated framework.[28] Comparison of powder patterns of solvated and activated $[Zn_2(ndc)_2(bpe)]$ with simulated powder patterns from single-crystal structures suggests that doubly interpenetrated $[Zn_2(ndc)_2(bpe)]$ converts to a triply interpenetrated structure upon activation (Figure S9), but the transformation does not appear to proceed as a SCPT.

When single-crystal to polycrystalline-phase transformations occur as the result of solvent removal, it is difficult to argue that the mechanism does not involve partial dissolution and regrowth of the components. However, such processes can be discounted in the case of single-crystal to single-crystal transformations, especially when the same crystal is used to determine the structures before and after conversion. We have shown that it is possible to change the degree of interpenetration of a three-dimensional MOF as a SCPT, and we have postulated a mechanism involving a concerted process of coordination bond cleavage and re-formation facilitated by transverse sliding of pillared layers. This study probes the limits to which a single-crystal material can undergo structural rearrangement while still maintaining the macroscopic integrity of the crystal a discrete entity.

## ■ ASSOCIATED CONTENT

### Supporting Information

Synthetic procedure, thermal analysis, detailed crystallographic information, additional figures, and an animation explaining the mechanism. This material is available free of charge via the Internet at http://pubs.acs.org.

## ■ AUTHOR INFORMATION


### Corresponding Author

ljb@sun.ac.za


### Notes

The authors declare no competing financial interest.

## ■ ACKNOWLEDGMENTS

We thank the National Research Foundation and the Claude Leon Foundation for financial support.

## ■ REFERENCES


(1) Tiekink, E. R. T., Vittal, J. J. *Frontiers in Crystal Engineering*; John Wiley & Sons, Ltd.: Chichester, 2006.

(2) Kobatake, S.; Takami, S.; Muto, H.; Ishikawa, T.; Irie, M. *Nature* **2007**, *446*, 778.

(3) Papaefstathiou, G. S.; Zhong, Z.; Geng, L.; MacGillivray, L. R. *J. Am. Chem. Soc.* **2004**, *126*, 9158.

(4) Inokuma, Y.; Yoshioka, S.; Ariyoshi, J.; Arai, T.; Hitora, Y.; Takada, K.; Matsunaga, S.; Rissanen, K.; Fujita, M. *Nature* **2013**, *495*, 461.

(5) Bernini, M. C.; Gándara, F.; Iglesias, M.; Snejko, N.; Gutiérrez-Puebla, E.; Brusau, E. V.; Narda, G. E.; Monge, M. Á. *Chem.—Eur. J.* **2009**, *15*, 4896.

(6) Jacobs, T.; Lloyd, G. O.; Gertenbach, J.-A.; Müller-Nedebock, K. K.; Esterhuysen, C.; Barbour, L. J. *Angew. Chem., Int. Ed.* **2012**, *51*, 4913.

(7) Takamizawa, S.; Nakata, E.-i.; Yokoyama, H.; Mochizuki, K.; Mori, W. *Angew. Chem., Int. Ed.* **2003**, *42*, 4331.

(8) Das, M. C.; Bharadwaj, P. K. *J. Am. Chem. Soc.* **2009**, *131*, 10942.

(9) Das, D.; Engel, E.; Barbour, L. J. *Chem. Commun.* **2010**, *46*, 1676.

(10) Li, H.; Eddaoudi, M.; O'Keeffe, M.; Yaghi, O. M. *Nature* **1999**, *402*, 276.

(11) Horike, S.; Shimomura, S.; Kitagawa, S. *Nat. Chem.* **2009**, *1*, 695.

(12) MacGillivray, L. R. *Metal–Organic Frameworks: Design and Application*; John Wiley & Sons, Inc.: New York, 2010.

(13) Yaghi, O. M.; O'Keeffe, M.; Ockwig, N. W.; Chae, H. K.; Eddaoudi, M.; Kim, J. *Nature* **2003**, *423*, 705.

(14) Maji, T. K.; Matsuda, R.; Kitagawa, S. *Nat. Mater.* **2007**, *6*, 142.

(15) Shekhah, O.; Wang, H.; Paradinas, M.; Ocal, C.; Schupbach, B.; Terfort, A.; Zacher, D.; Fischer, R. A.; Woll, C. *Nat. Mater.* **2009**, *8*, 481.

(16) Yang, S.; Lin, X.; Lewis, W.; Suyetin, M.; Bichoutskaia, E.; Parker, J. E.; Tang, C. C.; Allan, D. R.; Rizkallah, P. J.; Hubberstey, P.; Champness, N. R.; Mark Thomas, K.; Blake, A. J.; Schröder, M. *Nat. Mater.* **2012**, *11*, 710.

(17) Zhang, J.; Wojtas, L.; Larsen, R. W.; Eddaoudi, M.; Zaworotko, M. J. *J. Am. Chem. Soc.* **2009**, *131*, 17040.

(18) Prasad, T. K.; Suh, M. P. *Chem.—Eur. J.* **2012**, *18*, 8673.

(19) Ma, B.-Q.; Mulfort, K. L.; Hupp, J. T. *Inorg. Chem.* **2005**, *44*, 4912.

(20) Chun, H.; Dybtsev, D. N.; Kim, H.; Kim, K. *Chem.—Eur. J.* **2005**, *11*, 3521.

(21) Choi, S. B.; Furukawa, H.; Nam, H. J.; Jung, D.-Y.; Jhon, Y. H.; Walton, A.; Book, D.; O'Keeffe, M.; Yaghi, O. M.; Kim, J. *Angew. Chem., Int. Ed.* **2012**, *51*, 8791.

(22) Chen, B.; Liang, C.; Yang, J.; Contreras, D. S.; Clancy, Y. L.; Lobkovsky, E. B.; Yaghi, O. M.; Dai, S. *Angew. Chem., Int. Ed.* **2006**, *45*, 1390.

(23) Atwood, J. L.; Barbour, L. J.; Jerga, A.; Schottel, B. L. *Science* **2002**, *298*, 1000.

(24) Seo, J.; Bonneau, C.; Matsuda, R.; Takata, M.; Kitagawa, S. *J. Am. Chem. Soc.* **2011**, *133*, 9005.

(25) Zhang, J.-P.; Lin, Y.-Y.; Zhang, W.-X.; Chen, X.-M. *J. Am. Chem. Soc.* **2005**, *127*, 14162.

(26) Ohara, K.; Martí-Rujas, J.; Haneda, T.; Kawano, M.; Hashizume, D.; Izumi, F.; Fujita, M. *J. Am. Chem. Soc.* **2009**, *131*, 3860.

(27) Chen, B.; Ma, S.; Hurtado, E. J.; Lobkovsky, E. B.; Liang, C.; Zhu, H.; Dai, S. *Inorg. Chem.* **2007**, *46*, 8705.

(28) Chen, B.; Ma, S.; Zapata, F.; Lobkovsky, E. B.; Yang, J. *Inorg. Chem.* **2006**, *45*, 5718.

(29) Dybtsev, D. N.; Yutkin, M. P.; Peresypkina, E. V.; Virovets, A. V.; Serre, C.; Férey, G.; Fedin, V. P. *Inorg. Chem.* **2007**, *46*, 6843.

(30) Henke, S.; Schneemann, A.; Kapoor, S.; Winter, R.; Fischer, R. A. *J. Mater. Chem.* **2012**, *22*, 909.

(31) Liu, H.; Zhao, Y.; Zhang, Z.; Nijem, N.; Chabal, Y. J.; Zeng, H.; Li, J. *Adv. Funct. Mater.* **2011**, *21*, 4754.